Available online at www.sciencedirect.com
SCIENCE DIRECT®
Journal of volcanology and geothermal research
ELSEVIER
Journal of Volcanology and Geothermal Research 121 (2003) 83–98
www.elsevier.com/locate/jvolgeores

The bimodal pH distribution of volcanic lake waters

Luigi Marini *, Marino Vetuschi Zuccolini, Giuseppe Saldi

Dipartimento per lo Studio del Territorio e delle sue Risorse, Università di Genova, Corso Europa 26, 16132 Genova, Italy

Received 9 October 2001; received in revised form 24 July 2002; accepted 24 July 2002

Abstract

Volcanic lake waters have a bimodal pH distribution with an acidic mode at pH 0.5–1.5 and a near neutral mode at pH 6–6.5, with relatively few samples having pH 3.5–5. To investigate the reasons for this distribution, the irreversible water–rock mass exchanges during the neutralization of acid SO_4–Cl waters with andesite, under both low- and high-temperature conditions, were simulated by means of the EQ3/6 software package, version 7.2. Reaction path modeling under low temperature and atmospheric P_{CO_2} and f_{O_2}, suggests that several homogeneous and/or heterogeneous pH buffers exist both in the acidic and neutral regions, but no buffer is active in the intermediate, central pH region. Again, the same titration, under high-temperature, hydrothermal-magmatic conditions, is expected to produce comparatively infrequent aqueous solutions with pH values in the 3.5–5 range, upon their cooling below 100°C. Substantially different pH values are obtained depending on the cooling paths, either through boiling or conductive heat losses. These distinct pH values are governed by either HSO_4^- and $HCl_{(aq)}$, in poorly neutralized aqueous solutions, or the $CO_{2(aq)}/HCO_3^-$ couple and the P_{CO_2} value as well, in neutralized aqueous solutions. Finally, mixing of the acid lake water with the aqueous solutions produced through high-temperature titration and cooled below 100°C is unlikely to generate mixtures with pH values higher than 3, unless the fraction of the acidic water originally present in the lake becomes very small, which means its virtually complete substitution. Summing up, the evidence gathered through reaction path modeling of the neutralization of acid lake waters with andesite, both at low and high temperatures, explains the scarcity of volcanic lake waters with measured pH values of 3.5–5.

Keywords: volcanic lake water; pH; neutralization; water–rock interaction

1. Introduction

Long-term geochemical monitoring aimed at mitigating geological risks is carried out at some volcanic lakes, such as that on Ruapehu volcano, New Zealand (Giggenbach, 1974; Christenson and Wood, 1993; Christenson, 2000), Laguna Caliente on Poás volcano, Costa Rica (Brantley et al., 1987; Rowe et al., 1992; Martínez et al., 2000), Yugama Lake on Kusatsu–Shirane volcano, Japan (Takano and Watanuki, 1990; Ohba et al., 2000) and Lake Nyos (e.g. Kusakabe et al., 2000 and references therein). Numerous chemical data have been collected at Soufrière volcano, St Vincent, during the 1971–1972 eruption, when basaltic-andesite lavas were extruded subaqueously into the crater lake (Sigurdsson, 1977). Apart

* Corresponding author. Fax: +39-010-352169.
E-mail addresses: lmarini@dipteris.unige.it (L. Marini), zucco@dipteris.unige.it (M. Vetuschi Zuccolini).

0377-0273/02/$ – see front matter © 2002 Elsevier Science B.V. All rights reserved.
PII: S0377-0273(02)00413-4

Table 1
Compiled chemical analyses of crater lake waters

Lake name	Number of entries with pH	Minimum temperature (°C)	Maximum temperature (°C)	Minimum pH	Maximum pH	References
Albano	9	9.0	19.0	5.55	8.72	j, q
Averno	2	18.0	25.0	7.17	8.62	y
Bannoe	1	.	16.0	–	5.70	y
Batur	1	–	23.0	–	8.90	k
Bolsena	2	8.0	24.0	8.25	8.76	q
Bracciano	2	11.0	28.0	7.62	8.87	q
Crater Lake	1	–	9.0	–	7.00	k
Danau Segara Anak	1	–	21.0	–	7.10	a
Ebeku–Kuriles	1	–	26.0	–	2.60	y
Egon	1	–	15.0	–	2.20	w
El Chichón	12	28.3	56.0	0.56	2.87	b, e
Fogo	1	–	11.0	–	8.46	q
Furnas	2	13.0	13.0	7.10	7.34	q
Karymsky	10	5.5	56.0	3.20	7.20	m,y
Kawah Ijen	13	33.8	44.0	0.09	0.39	k, l
Kawah Putih	5	25.8	34.0	0.62	1.30	u
Keli Mutu	13	18.0	32.7	0.30	3.20	w
Kelut	1	–	41.0	–	5.90	k
Maly Semiachik	8	8.9	32.0	0.69	1.23	y
Martignano	2	7.0	8.0	7.53	8.04	q
Monoun	9	22.0	22.0	5.80	6.90	t
Monticchio Piccolo	12	6.6	9.3	6.28	7.03	f, g
Nemi	2	9.0	17.0	7.81	8.35	q
Nyos	12	22.2	26	5.10	8.10	c, k, n
Oyunuma	1	–	51.0	–	2.70	k
Pinatubo	5	36.7	46.5	1.90	4.79	y
Poás	4	44.0	87.0	−0.40	0.00	d, k, r
Popocatépetl	2	65.0	65.0	1.37	1.50	b
Quilotoa	10	13.3	13.9	6.34	7.60	a
Rincón de la Vieja	1	–	38.0	–	0.20	o
Ruapehu	31	15.0	65.6	0.60	1.20	h, i
Sete Cidades	2	13.0	13.0	7.86	7.93	q
Sirung	1	–	40.0	–	0.80	w
Soufrière St. Vincent	23	33.5	82.0	5.75	7.70	s
Taal	14	33.5	37.0	2.20	2.60	z
Vico	2	10.0	21.0	8.48	8.69	q
Wai Sano	2	28.0	28.0	3.00	3.10	w
Wum	1	–	25.0	–	8.10	p
Yakeyama	1	–	29.6	–	2.20	v
Yugama	32	7.8	33.0	0.90	1.80	v

References: (a) Aguilera et al. (2000); (b) Armienta et al. (2000); (c) Barberi et al. (1989); (d) Brantley et al. (1987); (e) Casadevall et al. (1984); (f) Chiodini et al. (1997); (g) Chiodini et al. (2000); (h) Christenson and Wood (1993); (i) Christenson (2000); (j) Cioni et al. (2002); (k) Delmelle and Bernard (1994); (l) Delmelle et al. (2000); (m) Fazlullin et al. (2000); (n) Giggenbach (1990); (o) Kempter and Rowe (2000); (p) Kusakabe et al. (1989); (q) Martini et al. (1994); (r) Rowe et al. (1992); (s) Sigurdsson (1977); (t) Sigurdsson et al. (1987); (u) Sriwana et al. (2000); (v) Takano and Watanuki (1990); (w) Varekamp and Kreulen (2000); (y) Varekamp et al. (2000); (z) Delmelle et al. (1998).

from a few examples at frequently monitored sites, most volcanic lakes have been the subject of single or a few geochemical surveys aimed at reconstructing their conceptual geochemical model and assessing geological risks. These different studies provide a relatively large amount of data that were recently compiled and interpreted by means of statistical and deterministic methods (Varekamp et al., 2000). It was shown that exotic fluids are commonly found in active crater lakes whereas dilute fluids generally occur in large caldera lakes. Lakes were grouped based on their main acidifying agents, either CO_2 or S compounds or $HCl+HF+H_2SO_4$. The acidity provided by these agents is variably neutralized by water–rock interaction, which represents the main source of cations. The present paper intends to revisit the water chemistry of volcanic lakes, focusing on pH distribution and the role of rock titration in controlling this pivotal variable.

2. Available data

A total of 255 chemical analyses of water, complete with pH values, from several volcanic lakes have been compiled (Table 1). The pH values have a bimodal frequency distribution with an acidic mode at pH 0.5–1.5 and a near neutral mode at pH 6–6.5, while only two samples, one from Pinatubo and one from Karymsky, have pH values between 3.5 and 5 (Fig. 1). The available data are heterogeneous, due to different strategies of sampling, and include time series, vertical profiles, or collection of a single sample, usually at the surface. There are many chemical analyses for a few lakes and single entries for other lakes. Since data are certainly not representative of pH distribution in volcanic lakes from a rigorously statistical point of view, questions concerning the frequency of the given pH classes are equivocal. However, the presence of an acidic mode and a near neutral mode with comparatively few samples in between the two modes is beyond doubt.

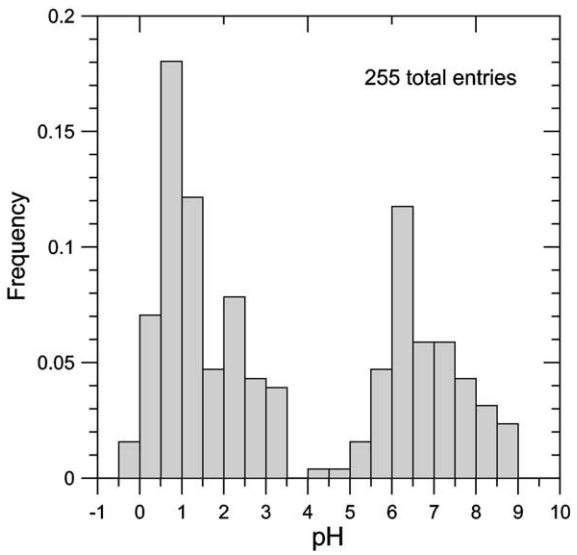

Fig. 1. Frequency distribution of pH of volcanic lake waters.

A similar, bimodal frequency distribution was observed for the pH of coal field waters (e.g. Cravotta et al., 1999 and references therein) and sulfide-mine drainages (e.g. Saldi, 2001; Marini et al., 2002). For instance, the coal-mine drainage in Pennsylvania has an acidic mode at pH 2.5–4 and a near neutral mode at pH 6–7 with few samples having pH 4.5–5.5 (Cravotta et al., 1999). Cravotta et al. (1999) attributed this pH frequency distribution to the relative progress of acid-generating pyrite weathering and acid-neutralizing calcite dissolution. These two reactions are reasonable pH-buffer candidates, due to their fast rates. Nevertheless, the dissolution of any carbonate, silicate, and hydroxide mineral is able to neutralize the acidity of natural waters.

3. Water chemistry of volcanic lakes

To gain more insight into the chemistry of volcanic lakes, pH is plotted against SO_4+Cl molalities in Fig. 2 (modified after Varekamp et al., 2000), in which acid SO_4–Cl waters, neutral SO_4–Cl waters, and neutral HCO_3 waters cluster in three separate groups. For any lake, water chemistry (including pH) is obviously controlled by input and output fluxes plus reaction contributions (e.g. Berner and Berner, 1996). Apart from evaporation and dilution effects, the chemistry of the acid SO_4–Cl lakes reflects inflow and absorp-

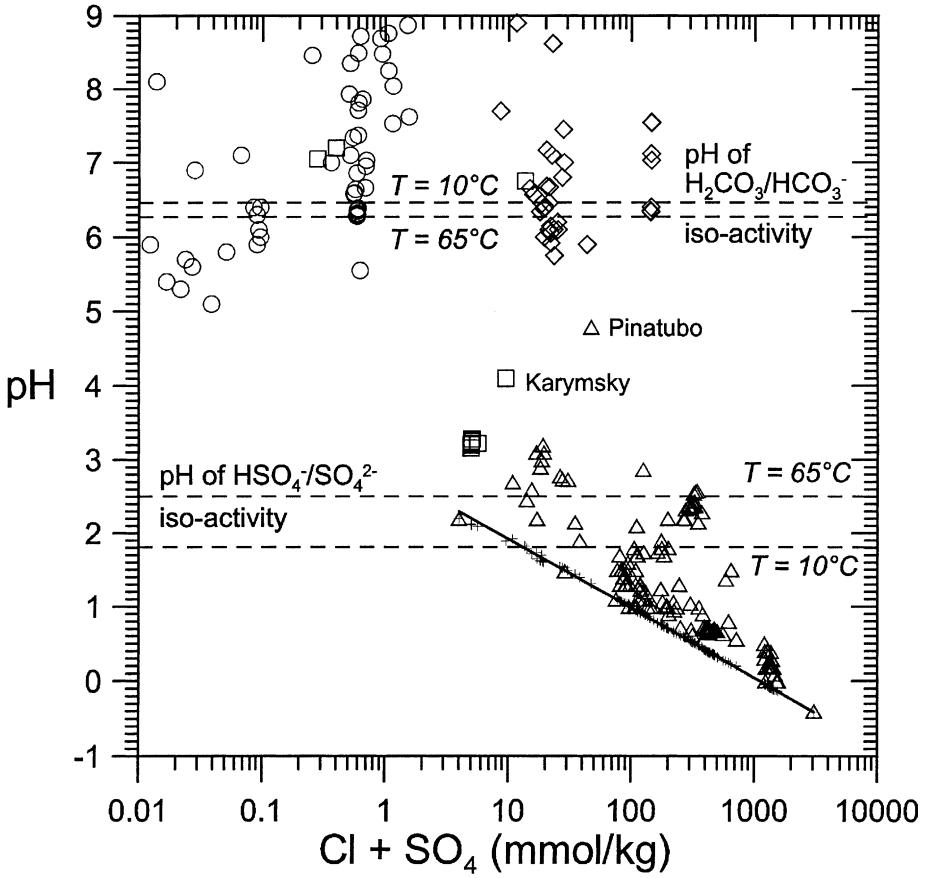

Fig. 2. Plot of pH vs. SO_4+Cl molalities for 255 volcanic lake waters. Explanation: triangles, acid SO_4–Cl waters; diamonds, neutral SO_4–Cl waters; circles, neutral HCO_3 waters; squares, data of Karymsky lake. The line with crosses indicates the initial compositions (before water–rock interaction) of acid, SO_4–Cl waters.

tion of volcanic gases rich in HCl, SO_2, and H_2S, whereas the neutral HCO_3 facies is controlled by input of gases rich in CO_2, of either mantle, metamorphic or organic (from decomposition of plants and animals) origin. Among the reaction terms, water–rock interaction (rock titration) plays a pivotal role both in acid SO_4–Cl lakes, where it brings about the neutralization of H_2SO_4, HSO_4^-, HCl, and HF, and in neutral HCO_3 lakes, where it determines conversion of aqueous CO_2 to HCO_3^-. Neutral SO_4–Cl waters from the Soufrière of St Vincent, Quilotoa, and Segara Anak lakes, can be considered to represent the product of virtually complete neutralization of acid SO_4–Cl solutions (Aguilera et al., 2000).

The reverse process occurred at Lake Karymsky at Academii Nauk volcano, Kamchatka, where a pH shift from ~7 to ~3.2 took place in less than 24 h in January 1996 due to a subaqueous eruption (Fazlullin et al., 2000). Dissolved carbonate species were quickly titrated to CO_2 by the acid species introduced in the lake and water composition changed from Na–HCO_3 to Na–SO_4. Of the ten compiled analyses, three have pH > 5, six have pH < 3.5, and only one has an intermediate pH of 4.1 (Fig. 2).

Fig. 2 shows that pH is strictly correlated with the sum of SO_4 and Cl molalities for acid SO_4–Cl lake waters, whereas these two variables are poorly correlated for neutral SO_4–Cl waters, and neutral HCO_3 waters. The strong pH–(SO_4+Cl) correlation for acid SO_4–Cl lakes stems from the

electroneutrality condition. In fact, in the absence of water–rock interaction, H^+ concentration (in equivalent units) must be equal to the sum of the concentrations of SO_4^{2-}, HSO_4^-, and Cl^-, i.e. the main anions.

4. The initial pH of acid SO_4–Cl waters

The initial pH of acid SO_4–Cl waters (i.e. pH in the absence of water–rock interaction) has been computed at the reported lake water temperature using the procedure of Varekamp et al. (2000), which assumes conservation of total SO_4 and Cl concentrations, based on:

(1) the two mass balances:

$$m_{Cl,T} = m_{HCl} + m_{Cl^-} \quad (1)$$

$$m_{SO_4,T} = m_{HSO_4^-} + m_{SO_4^{2-}} \quad (2)$$

(2) the two equilibrium constraints:

$$K_{Cl} = \frac{m_{Cl^-}\gamma_{Cl^-} m_{H^+}\gamma_{H^+}}{m_{HCl}\gamma_{HCl}} \quad (3)$$

$$K_S = \frac{m_{SO_4^{2-}}\gamma_{SO_4^{2-}} m_{H^+}\gamma_{H^+}}{m_{HSO_4^-}\gamma_{HSO_4^-}} \quad (4)$$

imposed by the dissociation of HCl and HSO_4^-, and

(3) the electroneutrality condition:

$$m_{Cl^-} + 2m_{SO_4^{2-}} + m_{HSO_4^-} = m_{H^+} \quad (5)$$

Activity coefficients of charged and neutral species were assumed to be equal to 1, although this is a rather crude approximation for ionic solutes in concentrated aqueous solutions. Through suitable substitutions, Eq. 5 can be put in the proton condition, obtaining:

$$-m_{H^+}^3 + m_{H^+}^2(-K_{Cl} - K_S + m_{SO_4,T}) +$$

$$m_{H^+}(-K_{Cl}K_S + 2m_{SO_4,T}K_S + m_{SO_4,T}K_{Cl} + m_{Cl,T}K_{Cl})$$

$$+m_{Cl,T}K_{Cl}K_S + 2m_{SO_4,T}K_{Cl}K_S = 0 \quad (6)$$

Uncertainties in the pH computed by means of Eq. 6 were checked for the two samples with the highest SO_4 and Cl concentrations, from Kawah Ijen and Poás, respectively, running speciation calculations by means of the software code EQ3NR (Wolery, 1992). The pH values computed by EQ3NR, −0.06 and −0.09, are not too far from the approximate values given by Eq. 6, −0.12 and −0.14, respectively.

As expected, the initial pH of acid SO_4–Cl waters and the corresponding sum of total SO_4 and Cl concentrations plot along a line in Fig. 2, as in Varekamp et al. (2000). Measured pH values are equal to or greater than initial pH values, indicating variable levels of neutralization by rock titration. Varekamp et al. (2000) defined: (1) the 'residual acidity' as the ratio between measured H^+ molality and initial H^+ molality, and (2) the 'degree of neutralization' as one minus the 'residual acidity'. These semi-quantitative classification parameters indicate the amounts of acid remaining and of acid consumed through rock dissolution, respectively, without specifying the degree of equilibration with individual minerals. Rock titration is expected to bring about an increase of pH at nearly constant SO_4+Cl, assuming negligible removal of SO_4 from the aqueous solution through precipitation of secondary sulfate minerals. The concentration of dissolved chloride, due to its conservative behavior, is expected to remain constant. Given this, why are there comparatively few samples of volcanic lake waters with pH of 3.5–5?

5. Reaction path modeling of acid SO_4–Cl waters neutralization

To answer this question, the irreversible water–rock mass exchanges during the neutralization of acid SO_4–Cl waters were simulated by means of the EQ3/6 software package, version 7.2 (Wolery, 1992; Wolery and Daveler, 1992), using the thermodynamic database COM. It includes the thermodynamic properties of several solids, aqueous species, and gases, which are mostly derived from SUPCRT92 (Johnson et al., 1992). The equilibrium constants of the hydrolysis reactions of jurbanite:

$$AlSO_4OH{\cdot}5\,H_2O + H^+ = Al^{3+} + SO_4^{2-} + 6\,H_2O \quad (7)$$

and ferrihydrite

$$Fe(OH)_{3(am)} + 3\,H^+ = Fe^{3+} + 3\,H_2O \quad (8)$$

were added to the existing database. Their log(K) values at 60°C, 1 bar were estimated to be −3.12 and 0.11 based on the available data at 25°C, 1 bar from Nordstrom (1982) and Langmuir (1997 and references therein), respectively. The van 't Hoff equation integrated for constant enthalpy of reaction was used for this purpose (e.g. Langmuir, 1997). The aqueous solution of Lake Poás, with 64 800 mg/kg total SO_4, 31 300 mg/kg total Cl, and EQ3-computed pH of −0.09 was chosen as representative of unreacted acid SO_4–Cl water (sample collected on January 8, 1987; Brantley et al., 1987). Reaction path modeling was performed by adding at each step of the reaction progress variable, ξ (Helgeson, 1979 and references therein), a corresponding amount of solid reactant to the system, and equilibrating at each step the aqueous solution with the possible product solid phases (Wolery and Daveler, 1992). An average andesite (Reed, 1997) was used as solid reactant and bulk dissolution, i.e. no constraint on the dissolution rates of primary solid phases, was assumed.

5.1. Titration at low temperature and atmospheric P_{CO_2} and f_{O_2}

First, rock–water interaction was simulated at constant temperature, 60°C, P_{CO_2}, $10^{-3.5}$ bar, and f_{O_2}, $10^{-0.78}$ bar, conditions that might be present throughout the lake if it is efficiently stirred by convection, although this is not always the case in natural systems.

Two separate runs were carried out. In the first run, the following solid phases were precipitated during water–rock interaction (in order of appearance): amorphous SiO_2, gypsum, jarosite, ferrihydrite, jurbanite, alunite, kaolinite, a montmorillonite solid mixture (made up of Mg, Ca, Na, and K endmembers), and a trigonal carbonate solid mixture (made up of calcite, rhodochrosite, and siderite). Solid mixtures were assumed to be ideal, since only this solid mixing model is supported by the EQ3/6 software package. This run is designed to estimate the ability of the system (aqueous solution plus secondary minerals) to resist pH variations upon rock titration. In a second run (see below) only gibbsite, amorphous SiO_2, and ferrihydrite were allowed to precipitate. In this run we test the buffer capacity of the aqueous solution with the minimum number of precipitating solid phases.

The selection of minerals involved in the first run could be criticized since most crater lake waters are only saturated in one or more silica minerals, gypsum, and barite, whereas many of the selected minerals are not observed in volcanic lakes (Varekamp et al., 2000). First, also natroalunite should be added to the list of the minerals that were observed to precipitate from crater lake waters, based on the evidence acquired at Yugama (Takano and Watanuki, 1990) and Ruapehu (Giggenbach, 1974). The natroalunite collected in a suspended sample at Ruapehu has stoichiometry $Na_{0.56}K_{0.44}Al_3(SO_4)_2(OH)_6$ with a weak prevalence of the Na-component over the K-component, i.e. alunite. Secondly, it is convenient to resume the analysis on the similarities between volcanic lake waters and mine waters (see above). In addition to the low pH values, acid mine waters and waters hosted in active volcanic lakes are also similar for their high concentrations of H_2SO_4 and related neutralization products, i.e. HSO_4^- and SO_4^{2-} ions. The obvious consequence of these similarities is the possible development of the same secondary minerals, such as several Al sulfates and Al hydroxi-sulfates variably hydrated (e.g. jurbanite, alunite, and basaluminite). These solid phases are less soluble than gibbsite and kaolinite and are expected to limit, therefore, Al concentrations in all natural sulfate-rich environments, at least at low–medium pH values (Nordstrom, 1982). Thirdly, it is instructive to compute the saturation indices of a typical acid lake water with respect to all relevant solid phases. This exercise was carried out by means of EQ3NR for the sample collected on May 10, 1996, from the Crater Lake of Mount Ruapehu (Christenson, 2000). The results (Table 2) show that this water is saturated not only with respect to silica miner-

als and anhydrite, as expected, but also with goethite and jarosite. In addition, taking the saturation index with respect to alunite (an observed secondary phase, see above) as a limit for the phases which might precipitate upon water–rock interaction, all the minerals appearing in Table 2, except pyrophyllite, should be considered as secondary minerals potentially forming during the incipient neutralization of acid crater lake waters.

The two titration curves of the acid SO_4–Cl water with andesite are shown in Fig. 3. Not surprisingly, rock titration involving precipitation of oxides, hydroxides, sulfates, silicates, and carbonates requires an amount of reactant larger than rock titration accompanied by production of $Al(OH)_3$, SiO_2, and $Fe(OH)_3$. In addition, the shape of the first curve is much more complicated than that of the second titration curve, due to the appearance and disappearance of several pH buffers, in analogy with what is observed by Reed (1997, see below). These pH buffers are constituted by coexistence of two or more solid phases with the aqueous solution, and are marked by nearly horizontal segments in Fig. 3. The first of these pH buffers is made up by jarosite, jurbanite, alunite and ferrihydrite, is active for ξ of 8.5–9.8 mol, and keeps pH at 1.65–1.66. As indicated by the following reaction:

$$\text{jarosite} + 3\ \text{jurbanite} + H_2O + \text{alunite} + 3\ \text{ferrihydrite} + 3\ SO_4^{2-} + 6\ H^+ \quad (9)$$

the coexistence of these solid phases fixes the pH, if SO_4^{2-} activity is nearly constant. Indeed, SO_4^{2-} activity varies slightly, from 2.09×10^{-2} to 2.14×10^{-2}, in this ξ range. The second pH buffer is more persistent than the previous one, for ξ values of 10.5–18.1 mol, it is constituted by jurbanite, kaolinite, and amorphous silica:

$$2\ \text{jurbanite} + 2\ \text{am.silica} = \text{kaolinite} + 7\ H_2O + 2\ SO_4^{2-} + 4\ H^+ \quad (10)$$

and it maintains pH in the interval 2.25–2.43. Again, it requires little change in SO_4^{2-} activity, which actually varies from 1.04×10^{-2} to 2.20×10^{-2}. The third pH buffer is even more durable, for ξ values of 18.9–31.0 mol, it is made up of alunite, kaolinite, amorphous silica, and montmorillonite:

$$\text{alunite} + \text{kaolinite} + 10\ SiO_2 + Mg^{2+} + H_2O = 3\ \text{K} - \text{montmorillonite} + 2\ SO_4^{2-} + 6\ H^+ \quad (11)$$

and controls pH values to 3.19–3.79. This buffer requires small changes in SO_4^{2-} activity (1.93×10^{-2} to 1.85×10^{-2}), in Mg^{2+} activity (1.34×10^{-1} to 4.87×10^{-3}), and in K-montmorillonite molar fraction (0.0041–0.25). The fourth pH buffer is active above ξ values of 33.4 mol, where pH is fixed at values ≥ 7.38 by saturation with respect to the trigonal carbonate solid mixture, mainly calcite:

Table 2
Saturation indices with respect to relevant solid phases for the water sample collected on May 10, 1996, from the Crater Lake of Mount Ruapehu; temperature 65.6°C; pH 0.99 (analytical data from Christenson, 2000)

Mineral	Chemical formula	log(Q/K)
Alunogen	$Al_2(SO_4)_3{\cdot}17\ H_2O$	−2.785
Alunite	$KAl_3(OH)_6(SO_4)_2$	−5.972
Anhydrite	$CaSO_4$	+0.052
Bassanite	$CaSO_4{\cdot}\frac{1}{2}H_2O$	−0.594
Chalcedony	SiO_2	+1.041
α-Cristobalite	SiO_2	+0.808
β-Cristobalite	SiO_2	+0.453
Epsomite	$MgSO_4{\cdot}7\ H_2O$	−1.834
Ferrihydrite	$Fe(OH)_3$	−4.293
Gibbsite	$Al(OH)_3$	−5.600
Glauberite	$Na_2Ca(SO_4)_2$	−5.507
Goethite	FeOOH	+0.354
Gypsum	$CaSO_4{\cdot}2\ H_2O$	−0.154
Hexahydrite	$MgSO_4{\cdot}6\ H_2O$	−3.248
Jarosite	$KFe_3(SO_4)_2(OH)_6$	+0.831
Jarosite–Na	$NaFe_3(SO_4)_2(OH)_6$	−5.921
Jurbanite	$Al(SO_4)(OH){\cdot}5\ H_2O$	−1.674
Kieserite	$MgSO_4{\cdot}H_2O$	−5.418
Mercallite	$KHSO_4$	−5.364
Pentahydrite	$MgSO_4{\cdot}5\ H_2O$	−3.584
Pyrophyllite	$Al_2Si_4O_{10}(OH)_2$	−6.371
Quartz	SiO_2	+1.280
SiO2(am)	SiO_2	+0.241
Starkeyite	$MgSO_4{\cdot}4\ H_2O$	−3.967
Syngenite	$K_2Ca(SO_4)_2{\cdot}H_2O$	−4.014
Thenardite	Na_2SO_4	−5.714

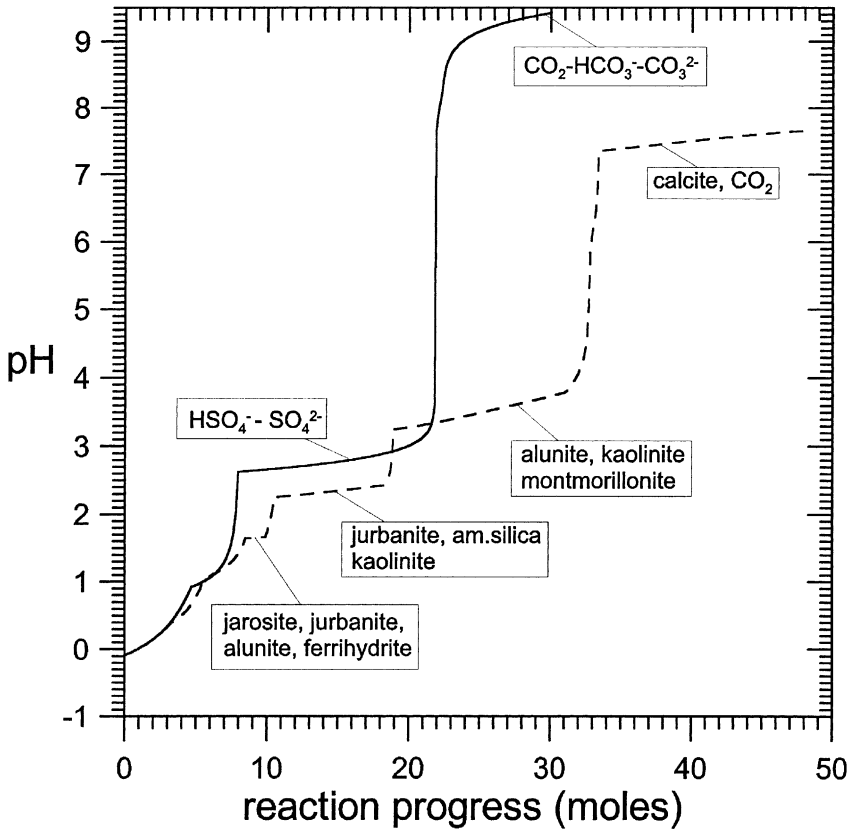

Fig. 3. Titration curves of the acid SO_4–Cl water of Lake Poás with an average andesite at 60°C, under open-system conditions with respect to CO_2 and O_2 and constant atmospheric P_{CO_2} and f_{O_2}. Explanation: dashed line (run 1), rock titration involving precipitation of oxides, hydroxides, sulfates, silicates, and carbonates; solid line (run 2), rock titration accompanied by precipitation of $Al(OH)_3$, SiO_2, and $Fe(OH)_3$

$$\text{calcite} + 2\,H^+ = Ca^{2+} + CO_2 + H_2O \qquad (12)$$

The second titration curve is characterized by the presence of two nearly horizontal segments (Fig. 3), delineating two pH buffers. The first one is active for ξ values of 7.9–20.8 mol, it fixes pH at 2.6–3.1, and it is controlled by the HSO_4^-/SO_4^{2-} couple, the optimum buffering capacity of which occurs at the pH of isoactivity, i.e. 2.44 at 60°C. The second pH buffer is active above pH 8.78, i.e. for $\xi \geq 23$ mol, and is governed by carbonate equilibria, involving mainly HCO_3^- and CO_3^{2-} ions and related complex species. Apart from the differences discussed above, both titration curves show large pH increases near the titration end-points, i.e. from pH 4 and 7 in the first case and pH 3 and 9 in the second one. In this central pH region no pH buffer exists and a small reaction progress, i.e. the addition of a small amount of rock, determines a large pH increment. In other words, pH in this central region is extremely unstable and can persist only for a limited time in the presence of reactive rocks. On the other hand, the unusual intermediate pH values might persist for a long time if the aqueous solution gets into contact with unreactive minerals and rocks, similar to what was observed in the geothermal reservoir of Tatun, which is chiefly developed within a 900-m thick sequence of orthoquartzitic sandstones (made up of quartz, kaolinite, and minor alunite, and elemental sulfur) and subordinately within highly altered andesites Truesdell (1991). However, this is a rare situation.

Of course, the pH values fixed by the carbonate

and sulfate buffers limiting the central pH region depend on the externally imposed conditions, i.e. temperature, P_{CO_2}, and f_{O_2}, but the pH of the titration end-point is expected to experience relatively small changes.

Fig. 3 also shows the non-linearity of the 'degree of neutralization' (Varekamp et al., 2000) with respect to ξ. For example, cogenetic fluids with a pH of about 3 buffered by alunite+kaolinite+montmorillonite would all have approximately the same 'degree of neutralization' value but distinct histories of water–rock reaction, with higher values of ξ going to the right.

5.2. Titration at high temperature and hydrothermal-magmatic P_{CO_2} and f_{O_2}

According to Varekamp et al. (2000), many crater lake fluids carry evidence of water–rock interaction at temperatures and pressures much higher than those present in lake settings. These crater lakes can be considered as the tops of the underlying hydrothermal-magmatic systems where water–rock interaction occurs prior to emergence to the surface. These deep processes of water–rock interaction were simulated by titrating the acid SO_4–Cl water of Lake Poás with the average andesite (see above) at 250°C and P_{H_2O} fixed by liquid–vapor coexistence. Carbon dioxide partial pressure was considered to be fixed at 2.63 bar by the P_{CO_2}–temperature relationship of Giggenbach (1984):

$$\log P_{CO_2} = 0.0168T - 3.78 \quad (13)$$

where P_{CO_2} is in bar and T is in °C. Since Eq. 13 applies to the full equilibrium condition among hydrothermal minerals and the aqueous solution, it might underestimate the P_{CO_2} values present in the roots of acid crater lakes. Oxygen fugacity was considered to be constrained at $10^{-31.28}$ bar by the H_2S–SO_2 magmatic gas buffer of Giggenbach (1987):

$$\log f_{O_2} = 5.924 - 19465/(T + 273.15) \quad (14)$$

which assumes that P_{H_2O} is controlled by vapor–brine coexistence. Although f_{O_2} is expected to decrease, upon progressive neutralization of the aqueous solution, towards values governed by the Fe(II)–Fe(III) hydrothermal buffer of Giggenbach (1987):

$$\log f_{O_2} = 10.736 - 25414/(T + 273.15) \quad (15)$$

redox conditions were maintained constant to keep the simulation to a reasonably simple level.

Progressive titration of the initially acid aqueous solution determines the separation of the following secondary solid phases (in order of appearance): pyrite, quartz, alunite, anhydrite, paragonite, hematite, muscovite, clinochlore, epidote, and albite. These minerals are typical constituents of the hydrothermal parageneses encountered in many explored geothermal systems (Henley and Ellis, 1983), hosting both neutral Na–Cl aqueous solutions and acidic SO_4–Cl to Cl–SO_4 waters. Moreover, these results are similar to those obtained by Reed (1997) for the reaction of the average andesite with diluted acidic, magmatic condensate (19 955 mg/kg SO_4, 13 643 mg/kg Cl, pH 0.79) at 300°C. Among these solid phases, pyrite and alunite have ephemeral existence and are totally consumed upon progression of water rock interaction. The final, stable mineral assemblage is made up of albite, anhydrite, clinochlore, epidote, hematite, muscovite, paragonite, and quartz. As already recognized by Reed (1997), the computed pH shows a step-by-step change with ξ (Fig. 4), from the initial value of 0.31 to the final value of 5.26, due to the action of different mineral buffers.

In natural systems the variably neutralized aqueous solutions experience substantial cooling, before entering the lake depression, from the hydrothermal temperatures to those of the lacustrine environment, which are obviously ≤ 100°C. The cooling processes through vapor separation (boiling) and conductive heat loss were modeled for selected aqueous solutions generated, during the titration of the acid SO_4–Cl water of Lake Poás with the average andesite at 250°C, for ξ values of 5–55 mol each 5 mol. Mixing of lake waters with the final hydrothermal solution ($\xi = 55$ mol) cooled in these two different ways was also modeled.

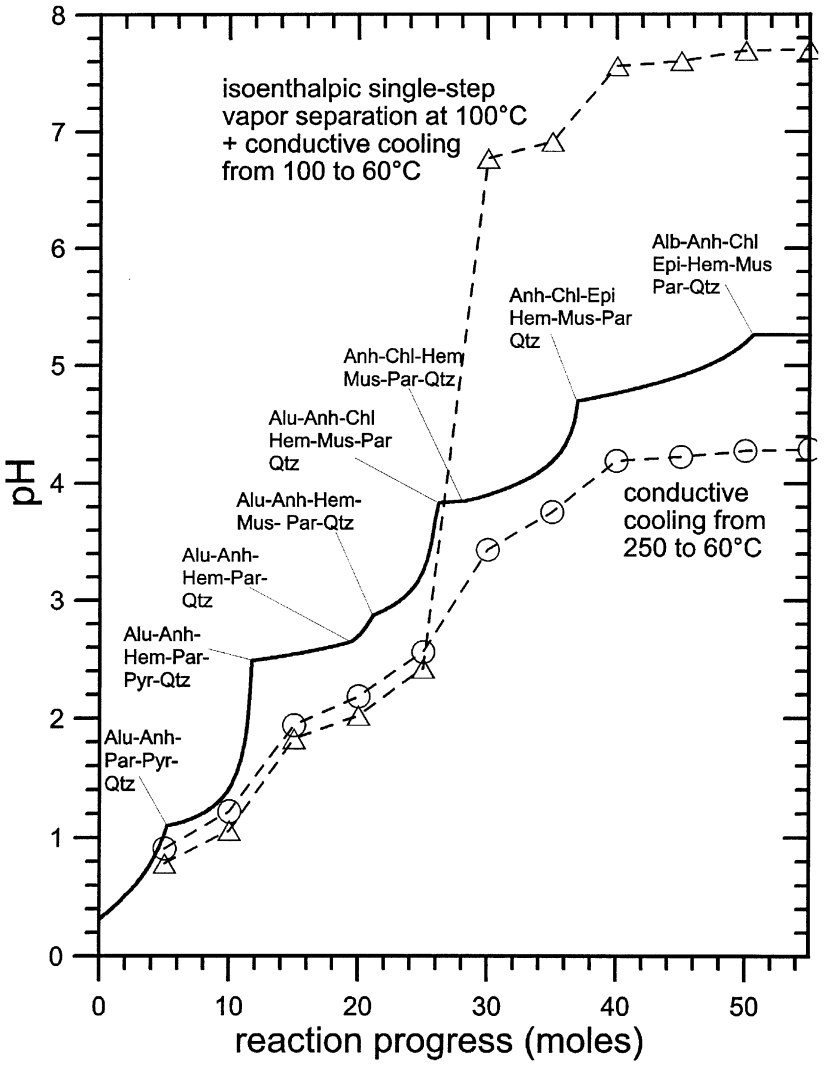

Fig. 4. Titration curve of the acid SO_4–Cl water of Lake Poás with an average andesite at 250°C, under open-system conditions with respect to CO_2 and O_2 and constant P_{CO_2} of 2.63 bar and f_{O_2} of $10^{-31.28}$ bar (solid line). The different mineral assemblages acting as pH buffers are indicated by means of the following abbreviations: Alb, albite; Alu, alunite; Anh, anhydrite; Chl, clinochlore; Epi, epidote; Hem, hematite; Mus, muscovite; Par, paragonite; Pyr, pyrite; Qtz, quartz. Also shown are the pH values of selected aqueous solutions produced during this titration process for ξ values of 5–55 mol, each 5 mol, cooled through either conductive cooling from 250 to 60°C (circles) or isoenthalpic single-step vapor separation at 100°C followed by conductive cooling from 100 to 60°C (triangles).

Since boiling cannot be modeled by means of EQ6, its effects were computed, assuming single-step vapor separation at 100°C and 1 bar, by means of the mass balances:

$$m_L = m_O/(1-y) \tag{16}$$

for non-volatile substances, and:

$$m_L = m_O/(1-y+yB_i) \tag{17}$$

for volatile substances. Subscripts O and L refer to the unboiled hydrothermal liquid and the separated liquid, respectively. Assuming isoenthalpic boiling the steam fraction, y, is given by:

$$y = (H_O - H_L)/(H_V - H_L) \quad (18)$$

where the H's are the specific enthalpies of the subscripted phases (V stands for vapor) under saturation conditions, i.e. coexistence of vapor and liquid (Keenan et al., 1969). The vapor–liquid distribution coefficient of the i-th volatile substance, $Bi = m_V/m_L$, at separation conditions, was obtained from the Henry's law constant, $K_{H,i}$, reported in the COM database of the EQ3/6 Software Package through the expression (Henley et al., 1984):

$$Bi = (K_{H,i} V_V)/(R\mathrm{T}) \quad (19)$$

where V_V is the specific volume of water vapor (Keenan et al., 1969), R is the universal gas constant and T is the absolute temperature. The vapor–liquid distribution coefficients at 100°C, 1 bar are 5026 for CO_2, 1609 for H_2S, 218.5 for SO_2 and 0.06534 for HCl. Hydrochloric acid has, therefore, a very low affinity for the vapor phase. Based on the computed concentrations of relevant constituents, the pH of the separated liquid phase at 100°C, 1 bar was calculated by means of EQ3NR, forcing H^+ molality through the electric balance and fixing Eh by the SO_4^{2-}/HS^- redox couple. Conductive cooling from 100 to 60°C, the same value of the low-temperature runs (see above), was then simulated by using EQ6. Obtained pH values at 60°C range from 0.79 to 2.42, for the aqueous solutions generated for ξ values of 5–25 mol, whereas the aqueous phases produced for ξ values of 30–55 mol have pH (at 60°C) of 6.77–7.70 (Fig. 4). The former ones experience small pH decreases (<0.8 pH units) upon boiling and conductive cooling, whereas the latter ones undergo large increases in pH (>2.4 units). This contrasting behavior reflects two very distinct aqueous environments, as already recognized by Reed (1991). Not surprisingly, the pH increase for ξ values ≥ 30 mol is due to CO_2 loss from an aqueous phase the pH of which is controlled by the $CO_{2(aq)}/HCO_3^-$ couple (Fig. 5a). On the other hand, the main aqueous acid species for $\xi \leq 25$ mol are, by far, HSO_4^- and $HCl_{(aq)}$. Since these acids are more associated at high temperature than at low, the temperature decrease drives to the right their dissociation reactions, thereby supplying to the aqueous solution more H^+ ions than those removed by loss of CO_2, which is a subordinate species in these environments.

The EQ6 code was used to simulate conductive cooling from 250 to 60°C. Computed pH values at 60°C range from 0.91 to 4.29 (Fig. 4) and are 0.1–1.0 pH units lower than the corresponding values at 250°C. Again, these decreases in pH with temperature reflect the changes in the dissociation constants of the weak acids present in the different aqueous solutions, which have high concentrations of HSO_4^- and $HCl_{(aq)}$ at low ξ values, and high concentrations of CO_2 and HCO_3^- at high ξ values (Fig. 5a). However, the constancy in the concentrations of all aqueous species upon cooling, including CO_2, prevents the large pH increase observed upon boiling for high ξ values.

The mixing processes between lake water (Poás sample collected on January 8, 1987; Brantley et al., 1987) and the final hydrothermal solution cooled at 60°C by either conductive cooling or boiling plus conductive cooling were simulated by means of EQ6. Amorphous silica is the only solid phase separated in significant amounts upon mixing for pH <3.1, whereas minor amounts of kaolinite, Na-saponite, jarosite, and ferrihydrite are produced at higher pH values. It must be underscored that pH values higher than 3.1 are attained only in mixtures very rich in the hydrothermal components, that is for fractions of this component greater than 0.999 (Fig. 6).

Summing up, the aqueous solutions generated through progressive neutralization of acid SO_4–Cl waters at 250°C have pH values ranging from 0.31 to 5.26. Conductive cooling of these waters to 60°C lowers their pH in the 0.91–4.29 range, whereas steam separation at 100°C followed by conductive cooling at 60°C determine pH values of 0.79–2.42 for poorly neutralized aqueous phases and of 6.77–7.70 for well neutralized aqueous solutions. Mixing of the final hydrothermal solutions cooled at 60°C with acidic lake waters rises the pH above 3.1 only when the fraction of the hydrothermal component is greater than 0.999, which means almost complete substitution of the acidic water present in the lake depression.

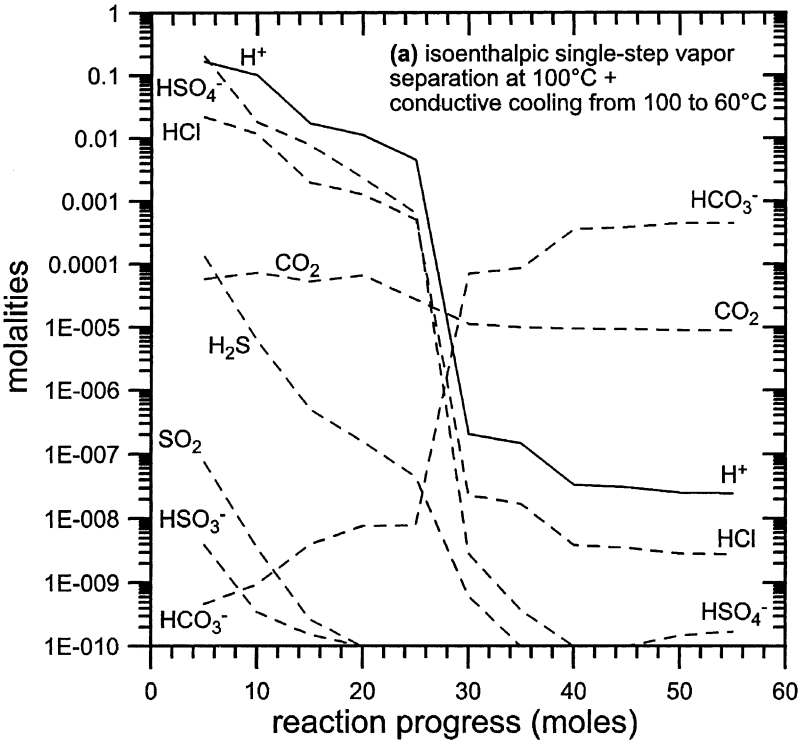
(a) isoenthalpic single-step vapor separation at 100°C + conductive cooling from 100 to 60°C
molalities
reaction progress (moles)
H+
HSO4-
HCl
HCO3-
CO2
H2S
SO2
HSO3-
1
0.1
0.01
0.001
0.0001
1E-005
1E-006
1E-007
1E-008
1E-009
1E-010
0
10
20
30
40
50
60

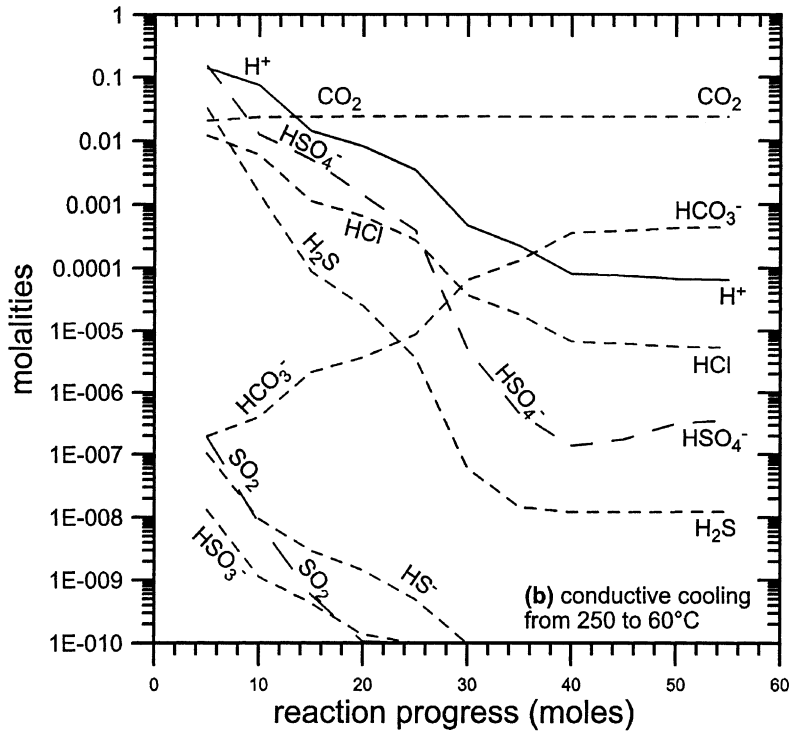
(b) conductive cooling from 250 to 60°C
molalities
reaction progress (moles)
H+
CO2
HSO4-
HCl
H2S
HCO3-
SO2
HSO3-
HS-
1
0.1
0.01
0.001
0.0001
1E-005
1E-006
1E-007
1E-008
1E-009
1E-010
0
10
20
30
40
50
60

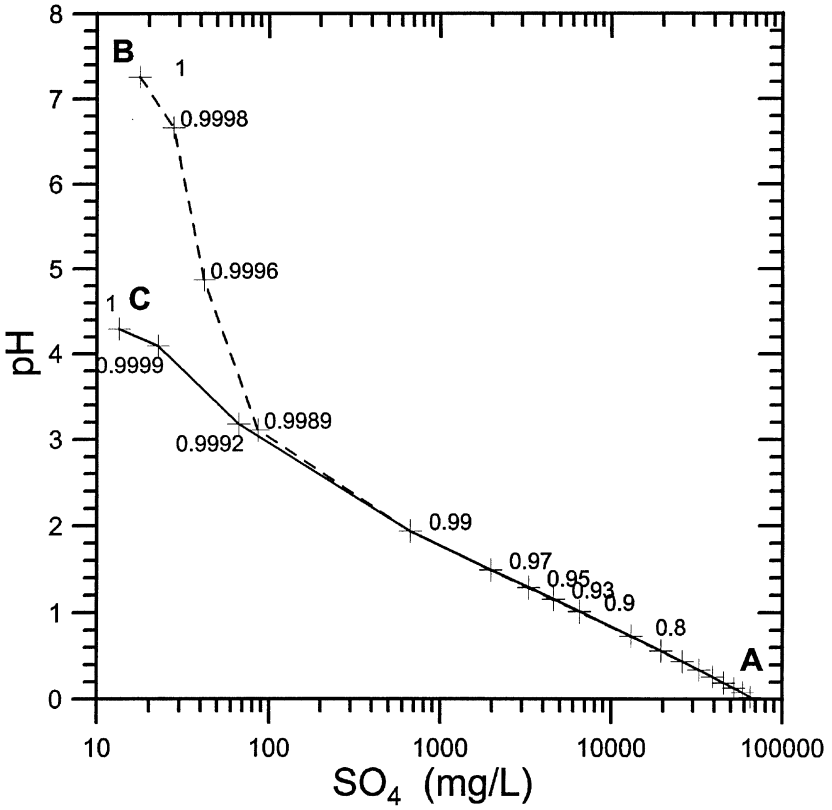

Fig. 6. Changes in SO_4 concentration and pH upon mixing of (A) the acid water of Lake Poás (temperature 60°C) with the hydrothermal water produced through complete neutralization of this acid SO_4–Cl water with an average andesite (at temperature of 250°C, P_{CO_2} of 2.63 bar and f_{O_2} of $10^{-31.28}$ bar) and cooled through either (B) isoenthalpic single-step vapor separation at 100°C followed by conductive cooling from 100 to 60°C, or (C) conductive cooling from 250 to 60°C. The numbers and crosses refer to the fractions of neutralized hydrothermal water in the mixture.

All in all, there is little doubt that aqueous solutions with intermediate pH values are not commonly produced even in this hydrologic framework.

6. Conclusions

Available pH data of volcanic lake waters have a bimodal frequency distribution with an acidic mode at pH 0.5–1.5 and a near neutral mode at pH 6–6.5, whereas few samples have a pH between 3.5 and 5. Although available data quality is heterogeneous, there is no doubt on the presence of these two modes.

The titration curves of acid SO_4–Cl water with andesite, obtained through reaction path modeling at low temperature, indicate that several homogeneous and/or heterogeneous pH buffers are active both in the acidic region and in the neutral region, whereas no buffer is present in the central pH region. Consequently, the addition of a small

Fig. 5. Molalities of H^+ ion and major dissolved acid species in selected aqueous solutions produced during the neutralization of the acid SO_4–Cl water of Lake Poás with an average andesite (at temperature of 250°C, P_{CO_2} of 2.63 bar and f_{O_2} of $10^{-31.28}$ bar) for ξ values of 5–55 mol, each 5 mol, cooled through either (a) isoenthalpic single-step vapor separation at 100°C followed by conductive cooling from 100 to 60°C, or (b) conductive cooling from 250 to 60°C.

amount of andesite, brings about a large increase in pH. In this central region, pH is highly unstable and can persist only for a short time in contact with reactive rocks.

Aqueous solutions with intermediate pH values are not commonly produced even through the neutralization of acid SO_4–Cl waters with andesite, under high-temperature, hydrothermal-magmatic conditions, followed by cooling below 100°C. Depending on the cooling process, either steam separation or conductive heat losses, very different pH values are obtained. They are controlled by either HSO_4^- and $HCl_{(aq)}$, in scarcely neutralized solutions, or the $CO_{2(aq)}/HCO_3^-$ couple and the P_{CO_2} value as well, in neutralized aqueous solutions.

Finally, also mixing of the acid lake water with the aqueous solutions generated by high-temperature titration and cooled below 100°C is unlikely to produce mixtures with pH values above 3, unless the fraction of the acid lake water becomes very small, which means its almost complete substitution.

In synthesis, the scarcity of volcanic lake waters with measured pH values of 3.5–5 is perfectly explained by the low- and high-temperature simulations of the neutralization of acid lake waters with andesite.

Acknowledgements

This paper greatly benefited from the editorial assistance by Margaret T. Mangan and the review by J.C. Varekamp, who provided data from his own database and suggested to simulate water–rock interaction at high temperature. An anonymous reviewer is also acknowledged for constructive comments.

References

Aguilera, E., Chiodini, G., Cioni, R., Guidi, M., Marini, L., Raco, B., 2000. Water chemistry of Lake Quilotoa (Ecuador) and assessment of natural hazards. In: Varekamp, J.C., Rowe, Jr., G.J. (Eds.), Crater Lakes. J. Volcanol. Geotherm. Res., 97, pp. 271–285.

Armienta, M.A., De la Cruz-Reyna, S., Macías, J.L., 2000. Chemical characteristics of the crater lakes of Popocatépetl, El Chichón, and Nevado de Toluca volcanoes, Mexico. In: Varekamp, J.C., Rowe, Jr., G.J. (Eds.), Crater Lakes. J. Volcanol. Geotherm. Res., 97, pp. 105–125.

Barberi, F., Chelini, W., Marinelli, G., Martini, M., 1989. The gas cloud of Lake Nyos (Cameroon, 1986): Results of the Italian technical mission. J. Volcanol. Geotherm. Res. 39, 125–134.

Berner, E.K., Berner, R.A., 1996. Global Environment: Water, Air, and Geochemical Cycles. Prentice Hall, Upper Saddle River, NJ.

Brantley, S.L., Borgia, A., Rowe, G., Fernandez, J.F., Reynolds, J.R., 1987. Poás volcano acts as a condenser for acid metal-rich brine. Nature 330, 470–472.

Casadevall, T.J., De La Cruz-Reyna, S., Rose, W.I., Bagley, S., Finnegan, D.L., Zoller, W.H., 1984. Crater lake and post-eruption hydrothermal activity, El Chichón volcano, Mexico. J. Volcanol. Geotherm. Res. 23, 169–191.

Chiodini, G., Cioni, R., Guidi, M., Marini, L., Principe, C., Raco, B., 1997. Water and gas chemistry of the Lake Piccolo of Monticchio (Mt. Vulture, Italy). Curr. Res. Volcan. Lakes 10, 3–8.

Chiodini, G., Cioni, R., Guidi, M., Magro, G., Marini, L., Raco, B., 2000. Gas chemistry of the Lake Piccolo of Monticchio, Mt. Vulture, in December 1996. Acta Vulcanol. 12, 139–142.

Christenson, B.W., 2000. Geochemistry of fluids associated with the 1995–1996 eruption of Mt. Ruapehu, New Zealand: Signatures and processes in the magmatic-hydrothermal system. In: Varekamp, J.C., Rowe, Jr., G.L. (Eds.), Crater Lakes. J. Volcanol. Geotherm. Res., 97, pp. 1–30.

Christenson, B.W., Wood, C.P., 1993. Evolution of a vent-hosted hydrothermal system beneath Ruapehu Crater Lake, New Zealand. Bull. Volcanol. 55, 547–565.

Cioni, R., Guidi, M., Raco, B., Marini, L., Gambardella, B., 2002. The water chemistry of Lake Albano (Italy) in December 1997. J. Volcanol. Geotherm. Res., in press.

Cravotta, III, C.A., Brady, K.B.C., Rose, A.W., Douds, J.B., 1999. Frequency distribution of the pH of coal-mine drainage in Pennsylvania. U.S. Geological Survey Toxic Substances Hydrology Program, Water Resources Investigation Report 99-4018A.

Delmelle, P., Bernard, A., 1994. Geochemistry, mineralogy, and chemical modeling of the acid crater lake of Kawah Ijen Volcano, Indonesia. Geochim. Cosmochim. Acta 58, 2445–2460.

Delmelle, P., Kusakabe, M., Bernard, A., Fischer, T., de Brouwer, S., del Mundo, E., 1998. Geochemical and isotopic evidence for seawater contamination of the hydrothermal system of Taal Volcano, Luzon, the Philippines. Bull. Volcanol. 59, 562–576.

Delmelle, P., Bernard, A., Kusakabe, M., Fischer, T.P., Takano, B., 2000. Geochemistry of the magmatic-hydrothermal system of Kawah Ijen volcano, East Java, Indonesia. In: Varekamp, J.C., Rowe, Jr., G.L. (Eds.), Crater Lakes. J. Volcanol. Geotherm. Res., 97, pp. 31–53.

Fazlullin, S.M., Ushakov, S.V., Shuvalov, R.A., Aoki, M.,

Nikolaeva, A.G., Lupikina, E.G., 2000. The 1996 subaqueous eruption at Academii Nauk volcano (Kamchatka) and its effects on Karymsky lake. In: Varekamp, J.C., Rowe, Jr., G.L. (Eds.), Crater Lakes. J. Volcanol. Geotherm. Res. 97, pp. 181–193.

Giggenbach, W.F., 1974. The chemistry of Crater Lake, Mt. Ruapehu (New Zealand) during and after the 1971 active period. N.Z. J. Sci. 17, 33–45.

Giggenbach, W.F., 1984. Mass transfer in hydrothermal alterations systems. Geochim. Cosmochim. Acta 48, 2693–2711.

Giggenbach, W.F., 1987. Redox processes governing the chemistry of fumarolic gas discharges from White Island, New Zeland. Appl. Geochem. 2, 143–161.

Giggenbach, W.F., 1990. Water and gas chemistry of Lake Nyos and its bearing on the eruptive process. In: Le Guern, F., Sigvaldason, G.E. (Eds.), The Lake Nyos event and natural CO_2 degassing, II. J. Volcanol. Geotherm. Res. 42, 337–362.

Helgeson, H.C., 1979. Mass transfer among minerals and hydrothermal solutions. In: Barnes, H.L.(Ed.), Geochemistry of Hydrothermal Ore Deposits. Wiley, New York, pp. 568–610.

Henley, R.W., Ellis, A.J., 1983. Geothermal systems, ancient and modern: A geochemical review. Earth Sci. Rev. 19, 1–50.

Henley, R.W., Truesdell, A.H., Barton, Jr., P.B., Whitney, J.A., 1984. Fluid-mineral Equilibria in Hydrothermal Systems. Reviews in Economic Geology, 1, 267 pp.

Johnson, J.W., Oelkers, E.H., Helgeson, H.C., 1992. SUPCRT 92: A software package for calculating the standard molal thermodynamic properties of minerals, gases, aqueous species, and reactions from 1 to 5000 bars and 0 to 1000°C. Comput. Geosci. 18, 899–947.

Keenan, J.H., Keyes, F.G., Hill, P.G., Moore, J.G., 1969. Steam tables. Thermodynamic properties of water including vapor, liquid, and solid phases (international system of units-S.I.). Wiley, 162 pp.

Kempter, K.A., Rowe, G.L., 2000. Leakage of Active Crater lake brine through the north flank at Rincón de la Vieja volcano, northwest Costa Rica, and implications for crater collapse. In: Varekamp, J.C., Rowe, Jr., G.L. (Eds.), Crater Lakes. J. Volcanol. Geotherm. Res., 97, pp. 143–159.

Kusakabe, M., Tanyileke, G.Z., McCord, S.A., Schladow, S.G., 2000. Recent pH and CO_2 profiles at Lakes Nyos and Monoun, Cameroon: Implications for the degassing strategy and its numerical simulation. In: Varekamp, G.J., Rowe, Jr., G.L. (Eds.), Crater Lakes. J. Volcanol. Geotherm. Res. 97, pp. 241–260.

Kusakabe, M., Ohsumi, T., Aramaki, S., 1989. The lake Nyos disaster: Chemical and isotopic evidence in waters and dissolved gases from three Cameroonian lakes, Nyos, Monoun, and Wum. J. Volcanol. Geotherm. Res. 39, 167–185.

Langmuir, D., 1997. Aqueous Environmental Geochemistry. Prentice Hall, Upper Saddle River, NJ.

Marini, L., Saldi, G., Cipolli, F., Ottonello, G., Vetuschi Zuccolini, M. 2002. Geochemistry of water discharges from the Libiola mine, Italy. Geochem. J., submitted.

Martini, M., Giannini, L., Prati, F., Tassi, F., Capaccioni, B., Iozzelli, P., 1994. Chemical characters of crater lakes in the Azores and Italy: The anomaly of Lake Albano. Geochem. J. 28, 173–184.

Martínez, M., Fernández, E., Valdés, J., Barboza, V., Van der Laat, R., Duarte, E., Malavassi, E., Sandoval, L., Barquero, J., Marino, T., 2000. Chemical evolution and volcanic activity of the active crater lake of Poás volcano, Costa Rica, 1993–1997. In: Varekamp, J.C., Rowe, Jr., G.L. (Eds.), Crater Lakes. J. Volcanol. Geotherm. Res. 97, pp. 127–141.

Nordstrom, D.K., 1982. The effect of sulfate on aluminum concentrations in natural waters: Some stability relations in the system Al_2O_3-SO_3–H_2O at 298 K. Geochim. Cosmochim. Acta 46, 681–692.

Ohba, T., Hirabayashi, J., Nogami, K., 2000. D/H and $^{18}O/^{16}O$ ratios of water in the crater lake at Kusatsu-Shirane volcano, Japan. In: Varekamp, G.J., Rowe, Jr., G.L. (Eds.), Crater Lakes. J. Volcanol. Geotherm. Res., 97, pp. 329–346.

Reed, M.H., 1991. Computer modeling of chemical processes in geothermal systems: examples of boiling, mixing, and water-rock reaction. In: D'Amore, F. (Ed.), Application of Geochemistry in Geothermal Reservoir Development. UNITAR, pp. 275–297.

Reed, M.H., 1997. Hydrothermal alteration and its relationship to ore fluid composition. In: Barnes, H.L. (Ed.), Geochemistry of Hydrothermal Ore Deposits. Wiley, New York, pp. 303–365.

Rowe, G.L.Jr., Ohsawa, S., Takano, B., Brantley, S.L., Fernandez, J.F., Barquero, J., 1992. Using crater lake chemistry to predict volcanic activity at Poás volcano, Costa Rica. Bull. Volcanol. 54, 494–503.

Saldi, G., 2001. Mappatura geochimica dell'entroterra di Chiavari-Sestri Levante mediante la caratterizzazione delle acque di falda e le acque acide della miniera di Libiola. Thesis, University of Genova.

Sigurdsson, H., 1977. Chemistry of the crater lake during the 1971–72 Soufrière eruption. J. Volcanol. Geotherm. Res. 2, 165–186.

Sigurdsson, H., Devine, J.D., Tchoua, F.M., Presser, T.S., Pringle, M.K.W., Evans, W.C., 1987. Origin of the lethal gas burst from Lake Monoun, Cameroun. J. Volcanol. Geotherm. Res. 31, 1–16.

Sriwana, T., van Bergen, M.J., Varekamp, J.C., Sumarti, S., Takano, B., van Os, B.J.H., Leng, M.J., 2000. Geochemistry of the acid Kawah Putih lake, Patuha Volcano, West Java, Indonesia. In: Varekamp, J.C., Rowe, Jr., G.L. (Eds.), Crater Lakes. J. Volcanol. Geotherm. Res., 97, pp. 77–104.

Takano, B., Watanuki, K., 1990. Monitoring of volcanic eruptions at Yugama crater lake by aqueous sulfur oxyanions. J. Volcanol. Geotherm. Res. 40, 71–87.

Truesdell, A.H., 1991. Origins of acid fluids in geothermal reservoirs. Geotherm. Res. Counc. Trans. 15, 289–296.

Varekamp, J.C., Kreulen, R., 2000. The stable isotope geochemistry of volcanic lakes, with examples from Indonesia. In: Varekamp, J.C., Rowe, Jr., G.L. (Eds.), Crater Lakes. J. Volcanol. Geotherm. Res., 97, pp. 309–327.

Varekamp, J.C., Pasternack, G.B., Rowe, G.L. Jr., 2000. Volcanic lake systematics II. Chemical constraints. In: Varekamp, G.J., Rowe, Jr., G.L. (Eds.), Crater Lakes. J. Volcanol. Geotherm. Res., 97, pp. 161–179.

Wolery, T.J., 1992. EQ3NR, A computer program for geochemical aqueous speciation-solubility calculations: Theoretical manual, user's guide and related documentation (version 7.0). Report UCRL-MA-110662 PT III. Lawrence Livermore National Laboratory, Livermore.

Wolery, T.J., Daveler, S.A., 1992. EQ6, A computer program for reaction path modeling of aqueous geochemical systems: Theoretical manual, user's guide, and related documentation (version 7.0). Report UCRL-MA-110662 PT IV. Lawrence Livermore National Laboratory, Livermore.